

# DFIG-Based Wind Power Conversion With Grid Power Leveling for Reduced Gusts

Vijay Chand Ganti, Bhim Singh, *Fellow, IEEE*, Shiv Kumar Aggarwal, and Tara Chandra Kandpal

**Abstract**—This paper presents a new control strategy for a grid-connected doubly fed induction generator (DFIG)-based wind energy conversion system (WECS). Control strategies for the grid side and rotor side converters placed in the rotor circuit of the DFIG are presented along with the mathematical modeling of the employed configuration of WECS. The proposed topology includes a battery energy storage system (BESS) to reduce the power fluctuations on the grid due to the varying nature and unpredictability of wind. The detailed design, sizing, and modeling of the BESS are given for the grid power leveling. Existing control strategies like the maximum power point extraction of the wind turbine, unity power factor operation of the DFIG are also addressed along with the proposed strategy of “grid power leveling.” An analysis is made in terms of the active power sharing between the DFIG and the grid taking into account the power stored or discharged by the BESS, depending on the available wind energy. The proposed strategy is then simulated in MATLAB-SIMULINK and the developed model is used to predict the behavior. An effort is made to make the work contemporary and unique, compared to the existing literature related to issues governing grid fed DFIG-based WECS.

**Index Terms**—Battery energy storage system (BESS), doubly fed induction generator (DFIG), grid power leveling, vector control, wind energy conversion system (WECS).

## I. INTRODUCTION

THE use of renewable sources for electric power generation has experienced a huge face lift since the past decade. Increased economical and ecological woes have driven researchers to discover newer and better means of generating electrical energy. In this race, wind energy conversion systems (WECS) have stood ahead of other renewable energy sources like solar energy, which still lags behind owing to high cost per kilowatt-hour (kWh) of electrical power generated. Overall, the contribution of these renewable energy systems to the power system has been increased rapidly from the last two decades [1]. Among all the available technologies for WECS, the doubly fed induction generator (DFIG) is most accepted because it combines the advantages of reduced converter ratings for power conversion and an efficient power capture due to the variable speed operation.

Manuscript received June 28, 2010; revised March 25, 2011; accepted July 06, 2011. Date of current version December 16, 2011.

V. C. Ganti and B. Singh are with the Department of Electrical Engineering, Indian Institute of Technology Delhi, New Delhi, 110016, India (e-mail: ganti.chand@gmail.com; bhimsinghiitd@gmail.com).

S. K. Aggarwal and T. C. Kandpal are with the Centre for Energy Studies, Indian Institute of Technology Delhi, New Delhi, 110016, India (e-mail: shiv3286@gmail.com; tck.studentinteraction@gmail.com).

Digital Object Identifier 10.1109/TSTE.2011.2170862

Variable speed operation of electric generators is arguably more advantageous [2], [3] compared to the fixed speed counter parts (using asynchronous generators without power electronic interface). The widely preferred topologies for the variable speed operation are the conventional asynchronous generators with rated power converters, the permanent magnet synchronous generators (PMSG's) with rated power converters, and the DFIG with partial rating power converters (slip power rating).

Among these, a WECS integrated with a DFIG is the most popular option to harness wind energy due to varying nature and unpredictability of the wind speeds. A DFIG-based WECS offers advantages of improved efficiency, reduced converter rating, reduced cost and losses, easy implementation of power factor correction, variable speed operation, and four quadrant control of active and reactive power control capabilities [4], [5]. Due to variable speed operation, total energy output is 20%–30% higher in case of DFIG-based WECS, so capacity utilization factor is improved and the cost per kWh energy is reduced.

Generally, the stator windings of the DFIG are directly connected to the grid and the rotor windings are fed through bidirectional PWM voltage source converters (VSCs) to control the rotor and stator output power fed to the grid for variable speed operation [6], [7]. It is possible to control rotor current injection using fully controlled electronic converters to ensure effective operation in both sub- and super-synchronous speed modes [6]. Decoupled control of active and reactive powers using the vector control is already discussed in detail by researchers [8], [9]. In a DFIG, both the stator and the rotor are able to supply active power, but the direction of this power flow through the rotor circuit is dependent on the wind speed and accordingly the generator speed. Below the synchronous speed, active power flows from the grid to the rotor side and rotor side converter (RSC) acts as the voltage source inverter while the grid side converter (GSC) acts as a rectifier but above the synchronous speed, RSC acts as the rectifier, and GSC acts as the inverter. The converter handles only around 25% of the machine rated power while the range of the speed variation is  $\pm 33\%$  around the synchronous speed [6]. An effective control strategy addresses the dynamics of a DFIG-based variable speed wind turbine and the operation of the converters under subsynchronous and super-synchronous modes of operation and during the transition period of these two modes.

Although, DFIG has proven to be a viable solution for high-performance WECS, grid connectivity is still a serious issue owing to the varying nature and unpredictability of wind speeds. The power output is highly fluctuating due to the same ( $\pm 100\%$

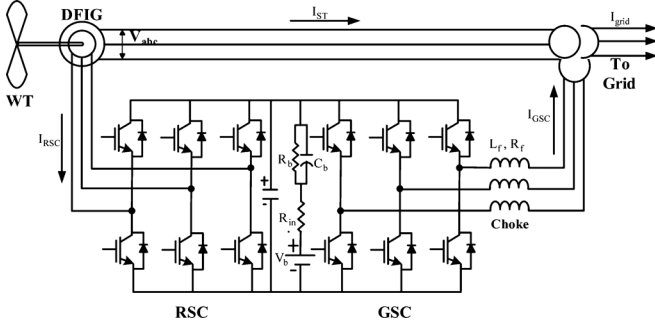


Fig. 1. DFIG-based WECS with a BESS (Thevenin's equivalent) in dc link for grid power leveling.

fluctuations on daily basis as shown in Fig. 2 and Table I and lower magnitude fluctuations in hours/minutes/seconds basis). Incorporating a battery or any other energy storage device in the dc link enables temporary storage of energy and, therefore, the ability to provide constant output active power, which is both deterministic and resistant to wind speed fluctuations [9]. This topology is explored in this paper and a novel control strategy to ensure “power-leveling” at the grid side is proposed. It can be argued over the selection of an energy storage system for higher rating WECS, but a detailed study on large-scale energy storage utilities is presented in [10]–[12]. Battery systems are employed for systems having ratings as high as 10 MW [13]. The WECS configuration used in this work (DFIG with converters cascade and a battery energy storage system (BESS) in the dc link) is shown in Fig. 1.

In this paper, a mathematical model for a grid connected DFIG is developed using back-to-back connected PWM-VSCs with a BESS in the dc link. Moreover, a detailed design procedure to select the rating of the BESS is also described by considering real-time data. The proposed “grid power leveling” control strategy is implemented in a stator flux oriented system, also taking into account other issues governing the satisfactory operation of a DFIG, viz., unity power factor operation of the machine, optimized active and reactive powers transfer, and tracking the maximum power point of the wind turbine.

## II. PROPOSED CONFIGURATION AND PRINCIPLE OF OPERATION

Fig. 1 shows a schematic of the DFIG with the rotor and grid side converters (RSC and GSC), a BESS in the dc link and a transformer and a choke (optional) in the rotor circuit. The BESS in the dc link is shown by its Thevenin equivalent [14], [15]. A configuration without the transformer in the rotor circuit (which accounts for the stator-rotor turns ratio of the DFIG) has also been reported in some literature. However, when the transformer is connected, the choke used for smoothening the currents of the GSC can be eliminated as the transformer leakage reactances would be sufficient enough for the cause. The rotor winding inductances act to smooth the currents of the RSC. This topology supports the complete control of the active and reactive powers of the system with the rotor and grid side converters around 33% (nearly one-third) of the rated speed [6]. Hence,

the converters used for this topology are to process only the slip power which is 25% to 35% of the overall machine rating.

The principle of operation of this topology for grid power leveling is that, by incorporating a battery in the dc link, a constant power is fed to the grid always. The average power for a given place (where the wind turbine is installed) is calculated from the available wind speeds and this calculated average power is fed to the grid to reduce the power fluctuations on the grid. At the higher wind speeds (and the machine operating at super-synchronous speed), power output of the WECS is higher as compared to the average power and, therefore, the extra power is stored in the battery. In contrast, at the lower wind speeds (and the machine operating at subsynchronous speed) the power is drawn from the battery to maintain the average power fed to the grid. Thus it is ensured that the power fed to the grid is always “leveled,” resulting in an efficient and reliable source of electrical power to the grid.

## III. DESIGN ISSUES IN PROPOSED WECS CONFIGURATION

Since wind energy is a nonreliable and unpredictable source of energy varying from time to time, stringent conditions are to be imposed in designing the proposed configuration of a WECS using DFIG with a BESS. Choosing the appropriate rating of the battery is of utmost importance as any discrepancy would lead to malfunctioning of the system. The major issues in designing the wind turbine and the BESS are as follows.

### A. Design of Wind Turbine

The output power of the turbine and the wind velocity has the nonlinear relation. The output power of the turbine is given by the following equation [16]:

$$P_m = 0.5 * C_p(\lambda, \beta) * \rho A v^3 \quad (1)$$

where  $C_p$  is power coefficient,  $\rho$  is air density,  $A$  is swept area of rotor blades,  $v$  is the wind-velocity,  $\lambda$  is the tip speed ratio, and  $\beta$  is the pitch angle.

The power coefficient is defined as the power output of the wind turbine to the available power in the wind regime. This coefficient determines the “maximum power” the wind turbine can absorb from the available wind power at a given wind speed. It is a function of the tip-speed ratio ( $\lambda$ ) and the blade pitch angle ( $\beta$ ). The blade pitch angle can be controlled by using a “pitch-controller” and the tip-speed ratio (TSR) is given as

$$\lambda = \frac{\omega R}{v} \quad (2)$$

where  $\omega$  is the rotational speed of the generator and  $R$  is radius of the rotor blades.

Hence, the TSR can be controlled by controlling the rotational speed of the generator. For a given wind speed, there is only one rotational speed of the generator which gives a maximum value of  $C_p$ , at a given  $\beta$ . This is the major principle behind “maximum-power point tracking” (MPPT) and a wind turbine needs to be designed keeping this strategy in mind.

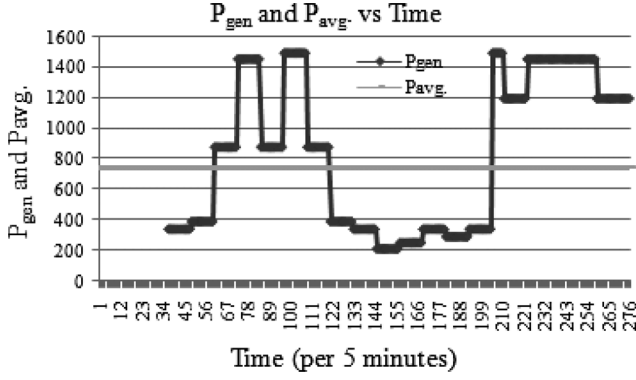


Fig. 2. Characteristics of the power generated ( $P_{gen}$ ) and average power ( $P_{avg}$ ) for a day.

### B. Design of BESS

As already explained, the design of a suitable rating of the BESS is very necessary for satisfactory operation of the proposed configuration of WECS. The rating of the BESS is decided by the total energy stored into it and this energy is stored for only those periods in which power generated by the machine is more than the average value that is to be fed to the grid. Initially, the average value of the power to be fed to the grid is calculated on the basis of the available wind speeds at that site. Knowing the value of this average power to be fed to the grid, the required rating of the battery bank ( $E_b$ ) is calculated as

$$E_b = \sum_{i=1}^n (P_{mi}) * t_i \quad (3)$$

where  $P_{mi}$  is the excess power at any instant (for every 5 min) than the average value of the power fed to the grid and  $t_i$  is the time period for which the excess power ( $P_{mi}$ ) is produced. ( $P_{mi}$  is in kW and  $E_b$  is in kWh.) These data are considered for each 5 min as shown in Fig. 2 from a practical site.

At any instant the value of  $P_{mi}$  can be calculated as

$$P_{mi} = (P_{inst} - P_{avg}) \quad (4)$$

where  $P_{inst}$  is the instantaneous power of the wind turbine and  $P_{avg}$  is the average active power to be fed to the grid.

The design of the battery bank is on the basis of the additional power produced for a whole day to minimize the fluctuations on the grid; therefore, wind speed data for a day is taken. Data for the wind speed is taken for a place Bapatla (Andhra Pradesh) situated in India on a day 11 November 2009 [17]. The wind speed is measured at a height of 20 m by using anemometers. But generally wind turbines are installed at a higher height. Therefore, the data of the wind speed must be calibrated in terms of the general height of the wind turbine installed, which is given as [18]

$$\frac{v}{v_o} = \left( \frac{h}{h_o} \right)^n \quad (5)$$

where  $v$  is new wind speed at a height  $h$ ,  $v_o$  is old wind speed at a height of  $h_o$ , and  $n$  is terrain factor.

A terrain factor ( $n$ ) of 0.13 is selected for the wind speed calibration in this paper. The power outputs of the DFIG-based WECS for the different wind speeds are given in Table I. The

TABLE I  
POWER GENERATED AT DIFFERENT WIND SPEEDS

| Time of the day | $V_o$ at $h_o$ | $V$ at $h$ | $P_{gen}$ (kW) |
|-----------------|----------------|------------|----------------|
| 12-1 A.M.       | 32.9           | 39.4       | 0              |
| 1-2 A.M.        | 28.3           | 33.9       | 0              |
| 2-3 A.M.        | 1.02           | 1.22       | 0              |
| 3-4 A.M.        | 5.14           | 6.2        | 340            |
| 4-5 A.M.        | 5.7            | 6.8        | 390            |
| 5-6 A.M.        | 12             | 9.8        | 880            |
| 6-7 A.M.        | 11.32          | 13.6       | 1460           |
| 7-8 A.M.        | 8.2            | 9.8        | 880            |
| 8-9 A.M.        | 12             | 14.3       | 1500           |
| 9-10 A.M.       | 8.2            | 9.8        | 880            |
| 10-11 A.M.      | 5.7            | 6.8        | 390            |
| 11-12 A.M.      | 5.14           | 6.2        | 340            |
| 12-1 P.M.       | 3.6            | 4.3        | 210            |
| 1-2 P.M.        | 4.2            | 5          | 250            |
| 2-3 P.M.        | 5.14           | 6.2        | 340            |
| 3-4 P.M.        | 4.6            | 5.5        | 290            |
| 4-5 P.M.        | 5.14           | 6.2        | 340            |
| 5-6 P.M.        | 12.35          | 14.8       | 1500           |
| 6-7 P.M.        | 10.3           | 12.3       | 1200           |
| 7-8 P.M.        | 11.32          | 13.6       | 1460           |
| 8-9 P.M.        | 11.32          | 13.6       | 1460           |
| 9-10 P.M.       | 11.32          | 13.6       | 1460           |
| 10-11 P.M.      | 10.3           | 12.3       | 1200           |
| 11-12 P.M.      | 10.3           | 12.3       | 1200           |

average power ( $P_{avg}$ ) is calculated from the power generated ( $P_{gen}$ ) for a day 11 November 2009, and it is found to be nearly 750 kW for that day. The averaging of the power can be done for a month or a whole year. A characteristic is shown between  $P_{gen}$ ,  $P_{avg}$ , and time of the day (per 5 min) in Fig. 2. It shows the periods in which power output is more than the  $P_{avg}$ . During these periods, the battery must store the additional power and is to be delivered to the grid at low wind speed periods to maintain the  $P_{avg}$  on the grid.

Accordingly, the rating of the battery bank is decided by using (3). In actual practice, it may be less than this value as the BESS is discharged in between too, as evident from Fig. 2.

The minimum voltage level of the battery bank is decided by the line voltage of the grid and is given as

$$V_{dc} = \left( \frac{N_2}{N_1} \right) \sqrt{\frac{2}{3}} V_{line} \quad (6)$$

where  $V_{dc}$  is the minimum required voltage of the battery bank, ( $N_2/N_1$ ) is the transformer turns ratio, and  $V_{line}$  is the line voltage on the grid side.

On the basis of the dc link voltage required ( $V_{dc}$ ), the total number of the batteries in the series ( $N_{series}$ ) are calculated as

$$N_{series} = \frac{V_{dc}}{V_b} \quad (7)$$

where  $V_b$  is the voltage of the single battery.

The number of the batteries required in the parallel ( $N_{\text{parallel}}$ ) are calculated as

$$N_{\text{parallel}} = \frac{E_b * 1000}{V_{\text{dc}} * P_b * \text{MDOD}} \quad (8)$$

where  $P_b$  is the capacity of the single battery in Ah and MDOD is the maximum depth of discharge of the battery, i.e., battery can be discharged only up to a maximum level generally, 80% for the Nickel-Cadmium batteries.

Thus a detailed and careful design of the BESS for a particular wind installation is to be performed.

#### IV. CONTROL STRATEGY

As shown in Fig. 3, the control strategy of the RSC and GSC consists of an “active and reactive power” controlling outer loop and the “current control” inner loop. A detailed explanation of the control strategy and the mathematical equations governing the same are presented below.

The exclusive control feature of the DFIG is that simultaneous and decoupled regulation can be made for active variables (speed, active power, or torque) and reactive variables (voltage, reactive power, or power factor). This can be achieved by developing the control algorithm in a two axis synchronously rotating reference frame, in which each axis takes care of either the active or reactive powers control. When the rotor power is allowed to flow in both directions, the control can be realized over a wide range of the rotor speeds, above and below and synchronous speed.

##### A. Control of GSC

The distinct feature of this work lies in modifying the active power outer loop of the GSC. The grid power is regulated to be a fixed value (determined by the average power as calculated earlier) and this is given as the reference active power. This is then compared with the actual grid power at any instant and the error is processed using a proportional-integral (PI) controller to generate the  $q$ -axis component of the reference grid current.

For the reactive power outer-loop control of the GSC, the controlled variable can be the stator reactive power. When it is controlled, the reactive power set point can be obtained in different ways depending on the power sharing strategy with the GSC. The desired reactive power sharing scheme (between the DFIG stator and the GSC) can be chosen, provided the total reactive power matches the requirement of the network ( $Q_{\text{total}} = Q_{\text{stator}} + Q_{\text{GSC}}$ ) and is within the operating limits.

The  $d$  and  $q$  components of the reference grid currents to be given to the PWM controller of the GSC are obtained from the reference active and reactive powers components.

The system considered in this work has both an active and a reactive powers loop. The active power loop of the system includes the grid power regulation to obtain “grid power leveling.” The reference reactive power ( $Q_{\text{ref}}$ ) can be set to zero for the unity power factor operation.

The expression for the reference  $q$ -axis grid current is as

$$i_{\text{gqref}} = \left( K_{\text{pp}} + \frac{K_{\text{ip}}}{s} \right) (P_{\text{gref}} - P_{\text{grid}}) \quad (9)$$

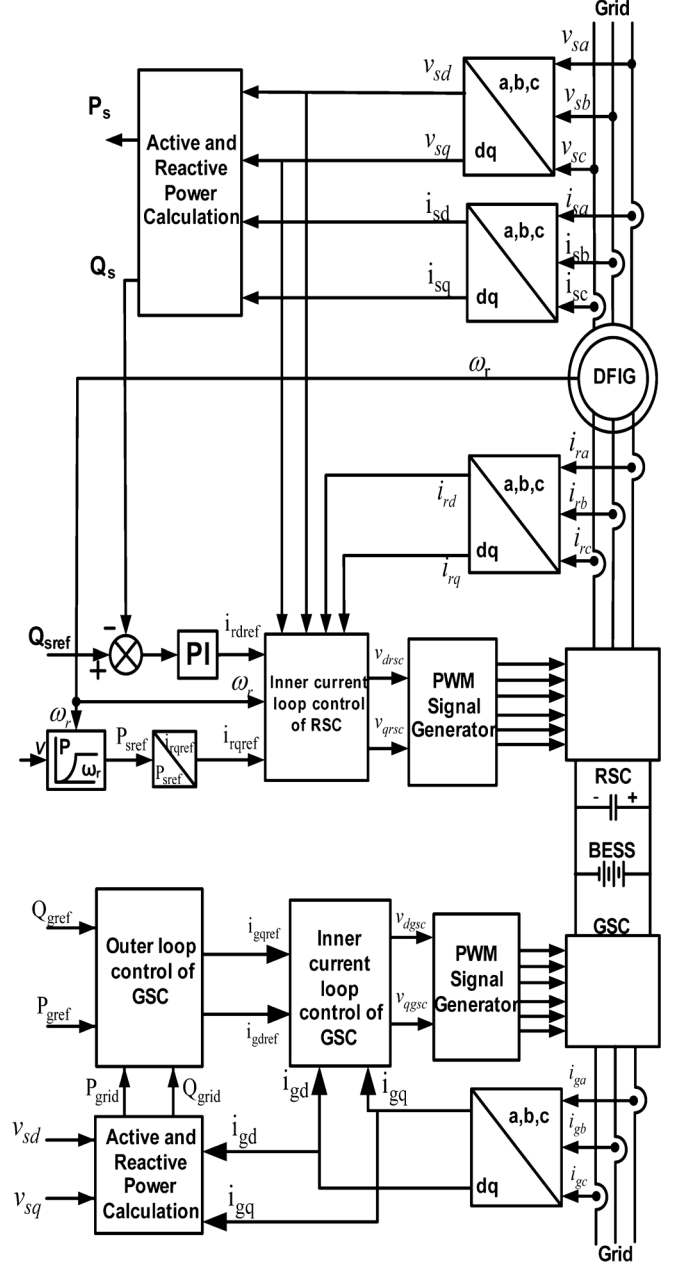


Fig. 3. Schematic diagram of proposed control strategy for RSC and GSC of a DFIG in a WECSS using BESS.

where  $K_{\text{pp}}$  and  $K_{\text{ip}}$  are the proportional and integral constants of the grid power regulator, respectively.

The reference  $d$ -axis grid current is chosen according to the reactive power sharing between the stator and the GSC, and it can be chosen to be zero, for a unity power factor operation.

These reference currents are then compared with the sensed grid side currents and the obtained error signal is processed with a PI controller to generate the control voltages for the PWM generator on the grid side. The expressions for the control voltages in  $d-q$  frame are given as

$$v_{\text{dgsc}} = \left( K_{\text{pgsc}} + \frac{K_{\text{igsc}}}{s} \right) (i_{\text{gdref}} - i_{\text{gd}}) \quad (10)$$

$$v_{\text{qgsc}} = \left( K_{\text{pgsc}} + \frac{K_{\text{igsc}}}{s} \right) (i_{\text{gqref}} - i_{\text{gq}}) \quad (11)$$

where  $i_{gd}$  and  $i_{gq}$  are the sensed  $d - q$  components of the grid currents and  $K_{pgsc}$  and  $K_{igsc}$  are the proportional and integral constants of the grid side current regulator respectively.

These control voltages are fed for PWM generation of the GSC, as shown in Fig. 3.

### B. Control of RSC

The RSC is a dedicated controller for the “machine” and hence the active and reactive power outer loops are chosen to extract the maximum power from the wind and to maintain a unity power operation of the stator. The active power set point can be obtained from the instantaneous value of the rotor speed and the rotor current  $i_{rq}$  is controlled in the stator flux-oriented reference frame to obtain the desired active power according to the optimum torque speed characteristics. The set point for the reactive power can be calculated from the active power set point and a desired power factor (considered to be unity in the present work). In the stator flux-oriented reference frame, the  $d$ -axis rotor current is used to control the required reference reactive power ( $Q_{sref}$ ).

The reference rotor currents ( $q$  and  $d$  components, respectively) are generated from the reference active and reactive power set points as

$$i_{rqref} = -\frac{L_s}{v_s L_m} P_{sref}, i_{rdref} = \frac{\phi_s}{L_m} - \frac{L_s}{v_s L_m} Q_{sref}. \quad (12)$$

These reference values of rotor currents are compared with the sensed values of rotor currents and the obtained error signal is processed with a PI controller to generate the control voltages for the PWM generator on the rotor side. The expressions for the control voltages in  $d - q$  frame are given as

$$v_{drsc} = \left( K_{prsc} + \frac{K_{irsc}}{s} \right) (i_{rdref} - i_{rd}) \quad (13)$$

$$v_{qrsc} = \left( K_{prsc} + \frac{K_{irsc}}{s} \right) (i_{rqref} - i_{rq}) \quad (14)$$

where  $i_{rd}$  and  $i_{rq}$  are the sensed  $d - q$  components of the rotor currents and  $K_{prsc}$  and  $K_{irsc}$  are the proportional and integral constants of the rotor side current regulator, respectively. These control voltages are fed for PWM generation of the RSC, as shown in Fig. 3.

## V. MATHEMATICAL MODELING OF DFIG

A simplified mathematical model would help in efficient analysis of the behavior of any complex system, under different operating conditions and control strategies. For a DFIG, the most common way of deriving a mathematical model is in terms of direct and quadrature axes ( $dq$  axes) quantities in a frame which rotates synchronously with the stator flux vector. An equivalent circuit for the DFIG in the synchronous reference frame [19] is represented in Fig. 4.

The expressions related to this model are as

$$v_{qds} = r_s i_{qds} + j\omega_e \psi_{qds} + \frac{d}{dt}(\psi_{qds})$$

$$v_{qdr} = r_r i_{qdr} + j\omega_e \psi_{qdr} + \frac{d}{dt}(\psi_{qdr})$$

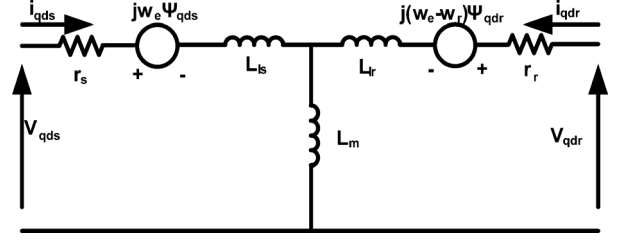


Fig. 4. Complex synchronous equivalent of a DFIG [19].

$$\begin{aligned} \psi_{qds} &= L_s i_{qds} + L_m i_{qdr} \\ \psi_{qdr} &= L_r i_{qdr} + L_m i_{qds} \\ T_e &= \frac{3p}{2} \text{Re}[j\psi_{qds} \cdot \overline{i_{qds}}] \\ &= \frac{3p}{2} \text{Re}[j\psi_{qdr} \cdot \overline{i_{qdr}}] \end{aligned} \quad (15)$$

where  $\overline{i_{qds}}$  and  $\overline{i_{qdr}}$  are the complex conjugates of the stator-current and rotor-current space vectors and stator and rotor inductances are defined as

$$L_s = L_{ls} + L_m \quad \text{and} \quad L_r = L_{lr} + L_m. \quad (16)$$

The complex torque equation of (15) can be resolved in reference  $d - q$  leading to

$$T_e = \frac{3p}{2} (\psi_{ds} \cdot i_{qs} - \psi_{qs} \cdot i_{ds}) = \frac{3p}{2} (\psi_{dr} \cdot i_{qr} - \psi_{qr} \cdot i_{dr}). \quad (17)$$

The stator side active and reactive powers are given as

$$\begin{aligned} P_s &= \frac{3}{2} \text{Re}[v_{qds} \cdot \overline{i_{qds}}] = \frac{3}{2} (v_{qs} i_{qs} + v_{ds} i_{ds}) \\ Q_s &= \frac{3}{2} \text{Im}[v_{qds} \cdot \overline{i_{qds}}] = \frac{3}{2} (v_{qs} i_{ds} - v_{ds} i_{qs}) \end{aligned} \quad (18)$$

considering that

$$\overline{i_{qds}} = \frac{1}{L_s} \overline{\psi_{qds}} - \frac{L_m}{L_s} \overline{i_{qdr}}. \quad (19)$$

The active and reactive power equations are modified as

$$\begin{aligned} P_s &= \frac{3}{2} \left\{ \frac{1}{L_s} (v_{qs} \psi_{qs} - v_{ds} \psi_{ds}) \right. \\ &\quad \left. - \frac{L_m}{L_s} \{ v_{qs} i_{qr} + v_{ds} i_{dr} \} \right\} \\ Q_s &= \frac{3}{2} \left\{ \frac{1}{L_s} (v_{qs} \psi_{qs} + v_{ds} \psi_{ds}) \right. \\ &\quad \left. - \frac{L_m}{L_s} (v_{qs} i_{dr} - v_{ds} i_{qr}) \right\}. \end{aligned} \quad (20)$$

Thus, the magnitudes of stator currents govern the active and reactive powers of the stator, and these currents depend on the rotor currents. Thus, the active and reactive powers can be controlled by appropriately controlling the rotor currents ( $i_{qr}$  and  $i_{dr}$ ) in WECS.

## VI. MATLAB-BASED MODELING

The MATLAB-based modeling of the proposed configuration of DFIG-based WECS with a BESS consists of a mechan-

ical system (wind turbine) and the electrical system (DFIG with back-to-back voltage source converters) and also the Thevenin's equivalent of a BESS.

#### A. Wind Turbine Modeling

The mechanical power output of the wind turbine is given by (1) and in that equation the power coefficient  $C_p(\lambda, \beta)$  is very important parameter. The power output of wind turbine is dependent on the power coefficient given as [20]

$$C_p(\lambda, \beta) = c_1 \left( \frac{c_2}{\lambda + c_8\beta} - \frac{c_2 c_9}{\beta^3 + 1} - c_3\beta - c_4\beta^{c_5} - c_6 \right) * e^{\left( \frac{-c_7}{\lambda + c_8\beta} + \frac{c_7 c_9}{\beta^3 + 1} \right)} + c_{10}\lambda \quad (21)$$

where  $\lambda$  is the tip speed ratio and given by the (2). The maximum value of  $c_p$  ( $c_{p \max} = 0.48$ ) is for  $\beta = 0$  degree and  $\lambda = 8.1$ . This particular value of  $\lambda$  is defined as the nominal value ( $\lambda_{\text{nom}}$ ). The coefficients used in (20) are given in Appendix A. The turbine parameters are given in Appendix B. The turbine parameters selected are for a 1.5-MW wind turbine manufactured by the Suzlon India Ltd. (S82) [21].

#### B. Battery Bank Design and Modeling

A detailed procedure to select the rating of the BESS was already mentioned in earlier sections. The MATLAB-based modeling of the battery is done using the Thevenin's equivalent of it as shown in Fig. 1. Since the battery is an energy storage unit, its energy is represented in kWh, when a capacitor is used to model the battery unit, the capacitance ( $C_b$ ) can be determined from

$$C_b = \frac{(\text{kWh}) \times 3600 \times 10^3}{0.5 (V_{\text{ocmax}}^2 - V_{\text{ocmin}}^2)} \quad (22)$$

where  $V_{\text{ocmin}}$  and  $V_{\text{ocmax}}$  are the minimum and maximum open circuit voltage of the battery under fully discharged and charged conditions. In the Thevenin's equivalent model of the battery,  $R_s$  is the equivalent resistance (external + internal) of parallel/series combination of a battery, which is usually a small value. The parallel circuit of  $R_b$  and  $C_b$  is used to describe the stored energy and voltage during charging or discharging.  $R_b$  in parallel with  $C_b$  represents self-discharging of the battery. Since the self-discharging current of a battery is small, the resistance  $R_b$  is large. The design details of the BESS used in this work are given in Appendix C.

#### C. Electrical System Modeling

The electrical system modeling is carried by using the sim power system toolbox of MATLAB-SIMULINK. The parameters of DFIG used in the model are given in Appendix D. The discussed control strategy is implemented on the RSC and the GSC. The developed model is tested for the proposed control strategy to achieve "grid power leveling" under different speeds of operation of the generator and the results are presented in detail in the next section.

### VII. RESULTS AND DISCUSSION

The model of WECS with BESS shown in Fig. 3 is developed in the MATLAB-SIMULINK as described in Section VI and re-

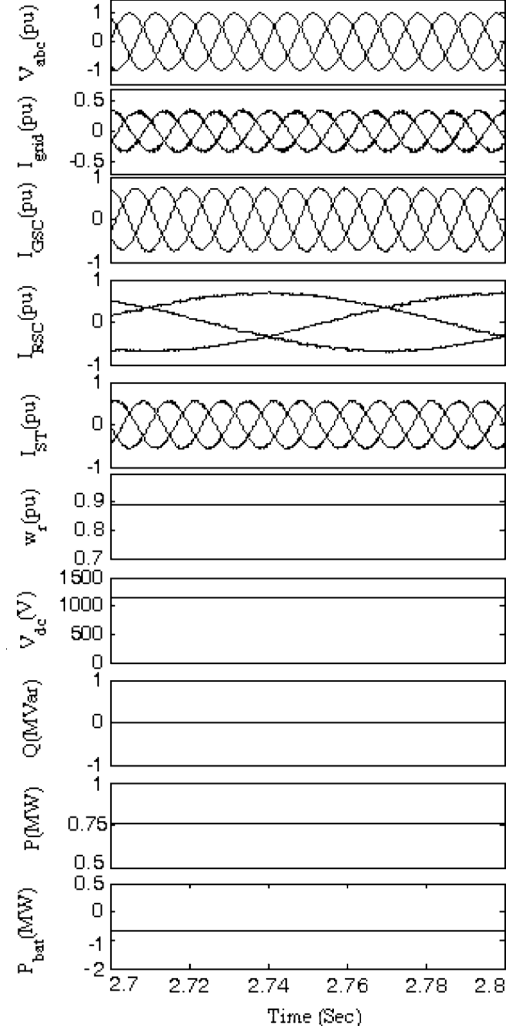


Fig. 5. Performance of a DFIG-based WECS with a BESS at subsynchronous speed (wind speed = 8 m/s, rotor speed = 0.9 p.u.).

sults are presented to demonstrate its behavior at different wind speeds.

Figs. 5, 6, and 7 show the performance of the proposed configuration of a DFIG-based WECS at subsynchronous speed, super-synchronous speed, and during transition i.e., at synchronous speed, respectively. The waveforms for stator voltage ( $V_{abc}$ ), grid current ( $I_{\text{grid}}$ ), grid side converter current ( $I_{\text{GSC}}$ ), rotor side converter current ( $I_{\text{RSC}}$ ), stator current ( $I_{\text{ST}}$ ), rotor speed ( $w_r$ ), dc link voltage ( $V_{\text{dc}}$ ), reactive power ( $Q$ ), grid power ( $P$ ), and battery power ( $P_{\text{bat}}$ ) are presented for different wind speeds. The convention for the battery power is chosen as to be negative if the battery discharges any power to the grid and positive if power is stored in the battery.

In all three cases, the value of the grid power is maintained to be constant at 0.75 MW by the modified grid power control strategy. However, this is maintained by either charging or discharging the battery in the corresponding region of operation. The reactive power is maintained at a stable value of zero, demonstrating a unity power factor operation. The analysis has been performed at variable wind speeds and the grid power is maintained to be constant at the reference value. The reference grid power can be chosen to be the average power supplied by

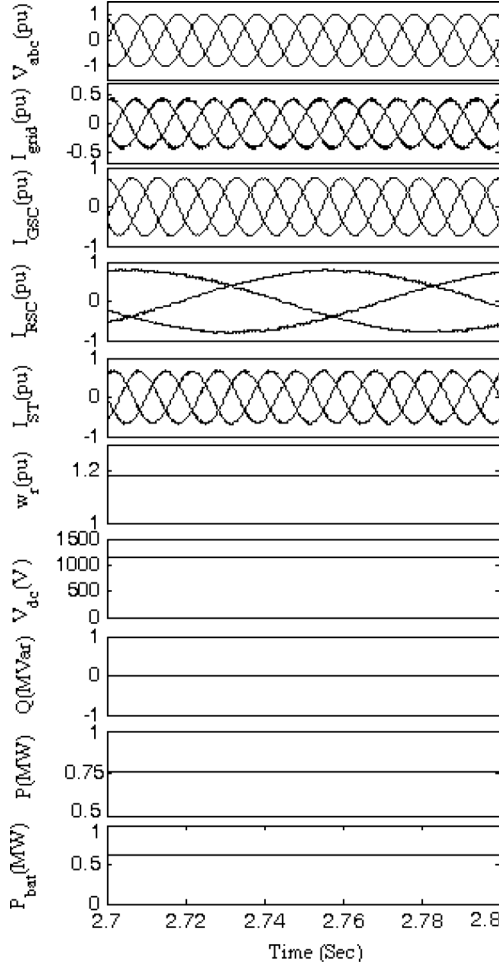


Fig. 6. Performance of a DFIG-based WECS with a BESS at super-synchronous speed (wind speed = 12 m/s, rotor speed = 1.2 p.u.).

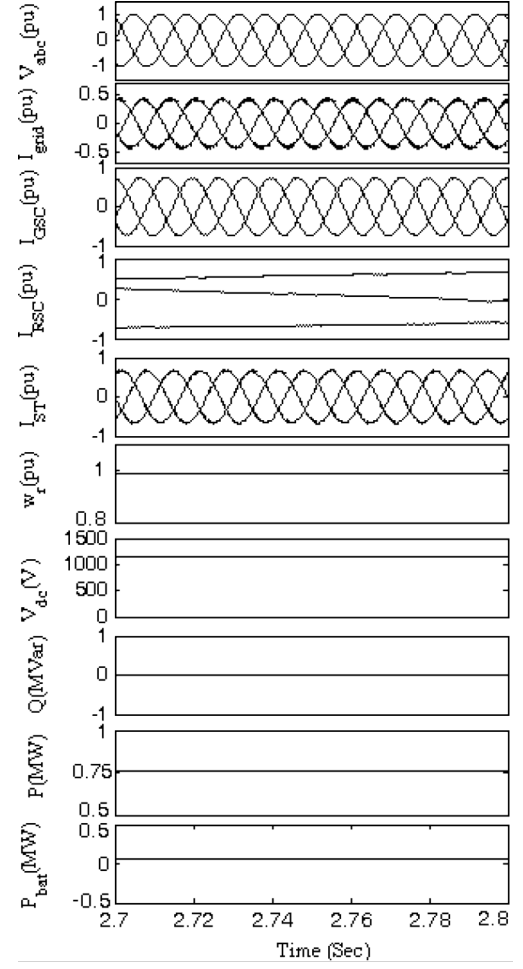


Fig. 7. Performance of a DFIG-based WECS with a BESS at synchronous speed (wind speed = 10 m/s, rotor speed = 1 p.u.).

the wind turbine to feed the constant power to the grid during the total period of operation. Hence, the grid power reference is chosen to be 0.75 MW as calculated and satisfactory results are obtained as shown in Figs. 5–7.

It can be argued over the results that, though the wind speed varies from a low to high during a given period of time, the power fed to the grid and hence the overall energy supplied to the grid, remains constant irrespective of these variations in wind speed. Thus the modified control strategy is able to negotiate the grid power gusts due to the variable wind speeds in an efficient way.

### VIII. CONCLUSION

A configuration of a DFIG-based WECS with a BESS in the dc link has been proposed with a control strategy to maintain the grid power constant. A methodology to design the BESS has been proposed by considering practical data at an installation point. The performance of the proposed control strategy on a DFIG-based WECS with BESS has been demonstrated under

different wind speeds. It has been observed that DFIG-based WECS with BESS demonstrates satisfactory performance under different wind speed conditions. This paper has also addressed the major disadvantage of connecting a DFIG to the grid, the “grid power gusts” due to the wind speed variations. If the utility fails to maintain the grid power constant, then during periods of “over-generation,” the consumers are to be paid in return to implement “load-leveling,” and absorb the excess power. This is an unbeneficial practice as the supplier loses both energy and money. The proposed configuration and control strategy, however, mitigates a need for this, by supplying a constant power to the grid throughout and thus maintaining a constant flow of energy to the grid irrespective of the variations in the wind speed. Moreover, other important control strategies like the maximum power point tracking (MPPT) and unity power factor operation at the stator terminal are also satisfactorily observed. Placing a BESS in the dc link of a DFIG-based WECS, proves to be a satisfactory implementation in terms of maintaining a constant power at the grid, set aside the disadvantages of using high rating of BESS.

## APPENDIX

A. Coefficients in the Empirical Expression for the Power Coefficient ( $C_p$ )

$c_1 = 0.5176, c_2 = 116, c_3 = 0.4, c_4 = 0, c_5 = 0, c_6 = 5, c_7 = 21, c_8 = 0.08, c_9 = 0.035$ , and  $c_{10} = 0.0068$ .

## B. Parameters of the Wind Turbine

| Parameter          | Value               |
|--------------------|---------------------|
| Rated Power        | 1500 kW             |
| Cut-in Wind Speed  | 4 m/s               |
| Rated Wind Speed   | 14 m/s              |
| Cut-out Wind Speed | 20 m/s              |
| No. of Blades      | 3                   |
| Rotor Diameter     | 82 m                |
| Swept Area         | 5281 m <sup>2</sup> |

## C. Parameters of the Battery

| Parameter (notation)                | Value    |
|-------------------------------------|----------|
| Battery Nominal Voltage ( $V_b$ )   | 1200 V   |
| Internal Resistance ( $R_b$ )       | 10000Ω   |
| Internal Capacitance ( $C_b$ )      | 675000F  |
| Battery Series Resistance ( $R_s$ ) | 0.00094Ω |

## D. Parameters of the DFIG

| Parameter (unit)                  | Value   |
|-----------------------------------|---------|
| Rated Power (MW)                  | 1.5     |
| Stator Voltage (V)/Frequency (Hz) | 575/50  |
| Stator/Rotor turns ratio          | 0.38    |
| Pole numbers                      | 4       |
| Stator Resistance (pu)            | 0.00706 |
| Rotor Resistance (pu)             | 0.005   |
| Stator leakage Inductance (pu)    | 0.171   |
| Rotor leakage Inductance (pu)     | 0.156   |
| Magnetizing Inductance (pu)       | 2.9     |
| Lumped Inertia Constant (s)       | 5.04    |

## REFERENCES

- [1] A. Miller, E. Muljadi, and D. Zinger, "A variable speed wind turbine power control," *IEEE Trans. Energy Convers.*, vol. 12, no. 2, pp. 181–186, Jun. 1997.
- [2] X. G. Wu, J. B. Ekanayake, and N. Jenkins, "Comparison of fixed speed and doubly-fed induction wind turbines during power system disturbances," in *Proc. Inst. Elect. Eng., Generation, Transmission and Distribution*, May 2003, vol. 150, no. 3, pp. 343–352.
- [3] S. S. Murthy, B. Singh, P. K. Goel, and S. K. Tiwari, "A comparative study of fixed speed and variable speed wind energy conversion systems feeding the grid," in *Proc. Int. Conf. on Power Electronics and Drive Systems (PEDS'07)*, 2007, pp. 736–743.
- [4] Y. Tang and L. Xu, "A flexible active and reactive power control strategy for a variable speed constant frequency generating system," *IEEE Trans. Power Electron.*, vol. 10, no. 4, pp. 472–478, Jul. 1995.
- [5] I. Boldea, *Variable Speed Generators*. New York: CRC Press, Taylor & Francis, 2006.
- [6] A. Tapia, G. Tapia, J. X. Ostolaza, and J. R. Saenz, "Modeling and control of a wind turbine driven doubly fed induction generator," *IEEE Trans. Energy Convers.*, vol. 18, no. 2, pp. 194–204, Jun. 2003.
- [7] L. Xu and Y. Wang, "Dynamic modeling and control of DFIG-based wind turbines under unbalanced network conditions," *IEEE Trans. Power Syst.*, vol. 22, no. 1, pp. 314–323, Feb. 2007.
- [8] R. Pena, J. C. Clare, and G. M. Asher, "A doubly fed induction generator using back to back PWM converters supplying an isolated load from a variable speed wind turbine," in *Proc. Inst. Elect. Eng., Electr. Power Appl.*, May 1996, vol. 143, no. 3, pp. 231–241.

- [9] L. Xu and W. Cheng, "Torque and reactive power control of a doubly fed induction machine by position sensorless scheme," *IEEE Trans. Ind. Appl.*, vol. 31, no. 3, pp. 636–642, May/Jun. 1995.
- [10] M. Black, V. Silva, and G. Strbac, "The role of storage in integrating wind energy," in *Proc. Int. Conf. Future Power Systems*, Nov. 16–18, 2005, pp. 1–6.
- [11] A. Nourai, "Large-scale electricity storage technologies for energy management," in *Proc. IEEE Power Eng. Soc. Summer Meeting*, 2002, vol. 1, pp. 310–315.
- [12] J. Eto, "Research, development and demonstration needs for large-scale reliability enhancing integration of distributed energy resources," in *Proc. 33rd Annu. Hawaii Int. Conf. Syst. Sci.*, Jan. 4–7, 2000, p. 2.
- [13] L. H. Walker, "10-MW GTO converter for battery peaking service," *IEEE Trans. Ind. Appl.*, vol. 26, no. 1, pt. 1, pp. 63–72, Jan./Feb. 1990.
- [14] Z. M. Salameh, M. A. Casacca, and W. A. Lynch, "A mathematical model for lead-acid batteries," *IEEE Trans. Energy Convers.*, vol. 7, no. 1, pp. 93–98, Mar. 1992.
- [15] B. Singh and G. K. Kasal, "Voltage and frequency controller for a three-phase four-wire autonomous wind energy conversion system," *IEEE Trans. Energy Convers.*, vol. 23, no. 2, pp. 509–518, Jun. 2008.
- [16] G. M. Masters, *Renewable and Efficient Electric Power Systems*. Hoboken, NJ: IEEE Press, Wiley-Interscience, 2004.
- [17] Hourly Wind Energy Data [Online]. Available: <http://www.imd.gov.in/section/nhac/aws/aws.htm>
- [18] T. Burton, D. Sharpe, N. Jenkins, and E. Bossanyi, *Wind Energy Handbook*. Chichester, England: Wiley, 2001.
- [19] M. G. Simoes and F. A. Farret, *Renewable Energy Systems: Design and Analysis With Induction Generators*. Orlando, FL: FI-CRC, 2004.
- [20] S. Heier, *Grid Integration of Wind Energy Conversion Systems*. Hoboken, NJ: Wiley, 1998.
- [21] Suzlon S82 Wind Turbine Brochure [Online]. Available: <http://www.suzlon.com/products/l2.aspx?l1=2&l2=8>



**Vijay Chand Ganti** was born in Visakhapatnam, India, in 1987. He received the B.Tech. (electrical and electronics) degree from Vignan's Institute of Information Technology, Visakhapatnam (affiliated with J.N.T.U., Hyderabad), in 2008 and the M.Tech. (power electronics, electrical machines and drives) degree from Indian Institute of Technology (IIT), Delhi, in 2010.

He is currently working as a research and design engineer in a reputed automobile company. His research interests include power electronics, electrical machines, electrical drives, renewable energy systems, and automotive drives control.



**Bhim Singh** (SM'99–F'10) was born in Rahamapur, India, in 1956. He received the B.E. (electrical) degree from the University of Roorkee, Roorkee, India, in 1977, and the M.Tech. and Ph.D. degrees from the Indian Institute of Technology (IIT) Delhi, New Delhi, India, in 1979 and 1983, respectively.

In 1983, he joined the Department of Electrical Engineering, University of Roorkee, as a Lecturer, and in 1988 became a Reader. In December 1990, he joined the Department of Electrical Engineering, IIT Delhi, as an Assistant Professor, where he became an Associate Professor in 1994 and Professor in 1997. Since September 2007, he has been ABB Chair Professor at IIT Delhi. His fields of interest include power electronics, electrical machines, electric drives, renewable energy generation, power quality, FACTS (Flexible AC Transmission Systems), and HVDC (High Voltage Direct Current) transmission systems.

Dr. Singh received the Khosla Research Prize of the University of Roorkee in 1991. He is a recipient of J. C. Bose and Bimal K Bose awards of The Institution of Electronics and Telecommunication Engineers (IETE) for his contribution in the field of power electronics. He is also a recipient of Maharashtra State National Award of the Indian Society for Technical Education (ISTE) in recognition of his outstanding research work in the area of power quality. He has received the PES Delhi Chapter Outstanding Engineer Award for the year 2006. He has been the General Chair of the IEEE International Conference on Power



Electronics, Drives and Energy Systems (PEDES'2006 and 2010) held in New Delhi. He has guided 36 Ph.D. dissertations, 120 M.E./M.Tech./M.S.(R) theses, and 60 BE/B.Tech. Projects. He is a Fellow of the Indian National Academy of Engineering (FNAE), The Institution of Engineering and Technology (FIET), The National Academy of Science, India (FNASc), Institution of Engineers (India) (FIE), and Institution of Electronics and Telecommunication Engineers (FIETE), and a Life Member of the Indian Society for Technical Education (ISTE), the System Society of India (SSI), and the National Institution of Quality and Reliability (NIQR).



**Shiv Kumar Aggarwal** was born in Faridabad, India, in 1986. He received the B.Tech. (electrical engineering) degree from the Kurukshetra University, Haryana, India, in 2007, and the M.Tech. degree from the Indian Institute of Technology (IIT) Delhi, New Delhi, India, in 2010.

His research area is developing new efficient converters for the renewable energy systems like wind, solar, and small hydro, etc.



**Tara Chandra Kandpal** received the Masters degree in physics from Kumaon University, Almora, in the Central Himalayan region of the state of Uttarakhand in India, in 1976, and the Ph.D. degree in solar energy from the Indian Institute of Technology Delhi, India, in 1980.

He has been a faculty member at the Centre for Energy Studies of the Indian Institute of Technology Delhi since 1981 and is currently a Professor of solar energy. His areas of primary research interest include optics of solar concentrators, testing and performance characterization of solar thermal devices and systems, techno-economics of renewable energy technologies, and renewable energy education and training. He has published over two hundred research papers in international journals of repute and conference proceedings in the above-mentioned research areas. He has also coauthored/coedited seven books in the area of renewable energy. He has also held several important administrative positions at the Indian Institute of Technology Delhi. He coordinated the United Nations University, Tokyo sponsored international training program at the Institute for participants from Africa and Asia for almost 13 years from 1987 to 2000. His other assignments include Vice Chairman, Joint Entrance Examination, Chairman, Graduate Aptitude Test in Engineering, Chairman, Joint Admission Test to M.Sc., Professor Incharge, Planning, and Secretary, Board of Educational Research and Planning of the Institute.

Dr. Kandpal was a United Nations University Fellow at the Brace Research Institute of McGill University, Montreal (Canada) for a period of one year during 1986–1987. He has guided about 20 doctoral students and many master level students for successful completion of their research work. He has been a recipient of the UNESCO/ROSTSCA Young Scientist Award for the year 1989 in the area of Energy Technology, is a Fellow of International Energy Foundation and a life member of Solar Energy Society of India and Indian Society for Technical Education. He has been and is a member of a large number of national committees relating to solar energy utilization in India. He has been a regular reviewer of research papers for most of the well-known international journals in the field of renewable energy. He has been an Editor of the *SESI Journal* (the research journal of the Solar Energy Society of India) during 1995–2001.